

**Revisited abundance diagnostics in quasars: Fe II/Mg II ratios**E. Verner<sup>1,2,3</sup> and F. Bruhweiler<sup>1,2,4</sup>D. Verner<sup>1,5</sup>S. Johansson<sup>6</sup>T. Gull<sup>2,7</sup>**ABSTRACT**

Both the Fe II UV emission in the 2000–3000 Å region (Fe II(UV)) and resonance emission line complex of Mg II at 2800 Å are prominent features in quasar spectra. The observed Fe II(UV)/Mg II emission ratios have been proposed as means to measure the buildup of the Fe abundance relative to that of the  $\alpha$ -elements C, N, O, Ne and Mg as a function of redshift. The current observed ratios show large scatter and no obvious dependence on redshift. Thus, it remains unresolved whether a dependence on redshift exists and whether the observed Fe II(UV)/Mg II ratios represent a real nucleosynthesis diagnostic. We have used our new 830-level model atom for Fe<sup>+</sup> in photoionization calculations, reproducing the physical conditions in the broad line regions of quasars. This modeling reveals that interpretations of high values of Fe II(UV)/Mg II are sensitive not only to Fe and Mg abundance, but also to other factors such as microturbulence, density, and properties of the radiation field. We find that the Fe II(UV)/Mg II ratio combined with Fe II (UV)/Fe II (Optical) emission ratio,

---

<sup>1</sup>IACS/Dept. of Physics, Catholic University of America.

<sup>2</sup>Laboratory of Astronomy and Solar Physics, NASA/Goddard Space Flight Center Greenbelt MD 20771.

<sup>3</sup>email: kverner@fe2.gsfc.nasa.gov

<sup>4</sup>email: fredb@iacs.gsfc.nasa.gov

<sup>5</sup>email: verner15@comcast.net

<sup>6</sup>Lund Observatory, Lund University, P.O. Box 43, S-22100 Lund, Sweden, sveneric.johansson@astro.lu.se

<sup>7</sup>email: Theodore.R.Gull@nasa.gov

where Fe II (Optical) denotes Fe II emission in 4000–6000 Å band, can be used as a reliable nucleosynthesis diagnostic for the Fe/Mg abundance ratios for the physical conditions relevant to the broad-line regions of quasars. This has extreme importance for quasar observations with the Hubble Space Telescope and also with the future James Webb Space Telescope.

*Subject headings:* atomic processes—line: formation—methods: numerical—quasars: emission lines

## 1. INTRODUCTION

The observed ratio of the ultraviolet Fe II UV emission flux (2000–3000 Å; hereafter Fe II (UV)) to that of the Mg II resonance doublet at 2800 Å in broad-line regions (BLRs) of quasars has a strong potential for being a fundamental cosmological metallicity indicator. In models of galactic chemical evolution, the ratio of Fe to  $\alpha$ -element (O, Ne, Mg) abundances constrains the ages of star-forming systems (Wheeler et al. 1989). The Fe/ $\alpha$  age constraint follows from a different enrichment timescale, namely:  $\alpha$ -elements are produced in supernova explosions of short-lived massive stars (primarily SN Type II), while Fe has a large contribution from the longer-lived intermediate-mass binaries that produce Type Ia supernovae. Predictions indicate that the Fe/ $\alpha$  abundance ratio should increase by more than an order of magnitude for stellar systems older than 1 Gyr (Hamann & Ferland 1993; Yoshii et al. 1996). However, if star formation has a significant contribution from very massive objects ( $100 < M_{\star} < 1000M_{\odot}$ ) as suggested recently (Heger & Woosley 2002), then substantial Fe production can occur at times earlier than 1 Gyr. The answer to whether the Fe/ $\alpha$  abundance ratio has a sharp break at 1 Gyr has important consequences not only for the evolution of the elements, but possibly for understanding the formation of active galactic nuclei (AGN) as well. Whether the Fe/ $\alpha$  enrichment is due to SN Ia or SN II explosions is a key problem to be addressed in constructing our picture of galactic evolution in the Early Universe.

The delay time in Fe enrichment can be estimated from observations by plotting the observed Fe II (UV)/Mg II emission ratio (or the Fe/Mg abundance) as a function of redshift. Recent Fe II (UV)/Mg II emission ratio measurements (e.g. Iwamuro et al. 2002; Dietrich et al. 2002; Freudling et al. 2003) show a wide range of values. That obscures any dependence on redshift. It is still unclear: (1) whether a dependence on redshift exists; and (2) whether the derived observed Fe II/Mg II values are sensitive to other physical parameters besides Fe abundance.

How the observed Fe II (UV)/Mg II emission ratio varies with physical conditions must be resolved before one can develop a reliable model that accurately predicts the Fe II emission line spectra in the BLRs of luminous AGNs. The large velocity dispersion of Fe II emission in BLRs, the large number of overlapping lines, and the overall richness of the Fe II spectrum (Verner et al. 1999) form broad emission blends, producing a "Fe II pseudo-continuum" and/or prominent features from the UV through visual (4000–6000 Å; hereafter Fe II (Optical)) to IR. This necessitates a complete simulation of the physical processes affecting the Fe<sup>+</sup> ion to deduce how the Fe II emission varies with properties of the radiation field, density, temperature, and Fe abundance in the emitting regions. To investigate what really makes Fe II emission strong in the rest-UV, we have used a new Fe<sup>+</sup> model ion. The model includes 830 atomic levels for Fe<sup>+</sup> (up to  $\approx 14$  eV) and represents an expansion of the previous model of Verner et al. (1999).

In this paper we evaluate how Fe II(UV)/Mg II and Fe II(UV)/Fe II(Optical) emission ratios vary due to extreme changes of the radiation field. Then, for the given density and radiation field, we investigate the Fe II emission properties within a reasonable range of Fe abundance and microturbulence.

## 2. EFFECTS OF PHYSICAL CONDITIONS ON Fe II EMISSION

### 2.1. The expanded Fe<sup>+</sup> ion model

Our earlier 371-level Fe<sup>+</sup> ion model (for energies below 11.6 eV), incorporated into the code CLOUDY<sup>8</sup>, predicts the emission fluxes of 68,635 Fe II lines (Verner et al. 1999). This 371-level model, plus accurate knowledge of the radiation field in a low-density plasma successfully predicted Fe II emission in the lower density environments of the Orion Nebula and Eta Carinae Ejecta (Verner et al. 2000; Verner et al. 2002). Comparison of observations with model results indicates that anomalously strong Fe II emission lines can be the result from line pumping due to coincidence of Fe II transitions with strong emission lines of other abundant ions (H I, He II, Si III, C IV, etc.; Hartman & Johansson 2000).

The higher radiation and particle density regimes in the BLRs of quasars favor the population of higher energy levels in Fe<sup>+</sup>. Consequently, we expanded the original Fe<sup>+</sup> model to 830 levels (energies below 14.06 eV yielding 344,035 transitions) and included more accurate atomic data – new experimental energy levels (Johansson 2002, private communication)

---

<sup>8</sup><http://pa.uky.edu/~gary/cloudy>

and A-values from the Amsterdam database<sup>9</sup> (see also Raassen & Uylings 1998). Where A-values were absent for many semi-forbidden transitions, and rate coefficients uncertain for Ly $\alpha$  pumping channels and primary cascades, we have inserted reasonable estimates.

The complete simulation of the physical processes affecting the Fe<sup>+</sup> ion makes it possible to deduce the density, temperature, plus predict iron abundance in the emitting regions. To accurately model the Fe II emission and Fe abundances, we must quantify the effects of the radiation field, and, only then, use Fe II(UV)/Mg II ratios to determine relative abundances. This approach is especially important for high redshift quasars where selection effects due to the luminosity may play a significant role. Thus, our knowledge about radiative excitation in Fe<sup>+</sup> is crucial to predict the Fe II spectrum and Fe abundances at high redshifts. The question is, "Can we use the observed Fe II(UV)/Mg II and Fe II(UV)/Fe II(Optical) ratios to derive Fe abundances?"

## 2.2. Model parameters and comparison of the 830 and 371-level models

In our modeling, we have chosen physical conditions where lines from low-ionization species like Fe II dominate the emission. We adopt a range of Fe abundance and a constant density,  $n_H = 10^{9.5} \text{ cm}^{-3}$ , with a total hydrogen column density,  $N_H = 10^{24} \text{ cm}^{-2}$ . We further assume that the flux of hydrogen ionizing photons at the illuminated face is  $10^{20.5} \text{ cm}^{-2} \text{ s}^{-1}$ . These parameters for BLR conditions are within the range of values taken from Verner et al. (1999), and Verner (2000). We employ the characteristic AGN continuum described in Korista et al. (1997), which consists of a UV bump peaking near 44 eV, a  $f_\nu \propto \nu^{-1}$  X-ray power law, and a UV to optical spectral index,  $a_{ox} = -1.4$ . For the adopted parameters, we have investigated how variations in abundance and microturbulence alter the intrinsic emission ratios of Fe II(UV)/Mg II and Fe II (UV)/Fe II(Optical).

The differences in the predicted Fe II spectrum calculated using 371 levels and 830 levels are negligible for lower densities and radiation field with depleted iron abundances (e.g. Orion Nebula). Differences in the predicted spectra from the two models become more significant with increased radiation field and iron abundance. Moreover, the shape of the radiation field in AGNs leads to increased population of higher energy levels in Fe II. Since densities are higher and the radiation field is more intense in BLRs, these upper levels provide additional excitation channels in the far UV (energies higher than 12 eV).

Figure 1 compares the predictions using our 371- and 830-level models for the Fe II

---

<sup>9</sup><ftp://ftp.wins.uva.nl/pub/orth/iron>

pseudo-continuum appropriate for BLR physical conditions in QSOs. The plotted spectra are given as flux versus wavelength, where flux is  $\nu f_\nu$ , in units of  $\text{erg cm}^{-2} \text{s}^{-1}$ . The comparison clearly shows how the increased number of atomic levels produces a stronger Fe II pseudo-continuum in QSO spectra. The 830-level ion model is far more accurate than the previous best efforts (Wills et al. 1985; Verner et al. 1999). The increased number of Fe<sup>+</sup> energy levels influences not only the Fe II spectrum but lines of other elements and the whole energy budget also. However, the complete study of the new theoretical emission spectrum is not a subject of this paper.

Table 1 shows the predicted Fe II(UV)/Mg II and Fe II(UV)/ Fe II(Optical) ratios for 830-level and 371-level models of Fe II versus contributions from the radiation field for a solar iron abundance and microturbulence of  $1 \text{ km s}^{-1}$ . The models were calculated for radiative continuum pumping and for pure collisional excitation. There is almost no change in predictions of 371-level and 830-level models for pure collisional excitation, if pumping by the radiation field is ignored. However, the predicted ratios are strongly influenced by the radiation field and are sensitive to contributions from the upper levels in Fe II. Figure 2 demonstrates the predicted Fe II spectrum due to collisions and radiative pumping.

### 2.3. Effects of microturbulence and abundance

How does the Fe II emission depend upon microturbulence? The first successful models were developed by Netzer & Wills (1983) who also demonstrated that the Fe II emission strength is sensitive to the turbulent velocity. This sensitivity was confirmed by modeling by Verner et al. (1999), who showed that the predicted UV Fe II emission indeed became stronger with increased microturbulence. To explore how microturbulence affects the observed Fe II(UV)/Mg II measurements, we calculated models with different microturbulence parameters ( $v_{turb} = 1, 5, 10, 100 \text{ km s}^{-1}$ ).

Figure 3 shows Fe II(UV)/Mg II and Fe II(UV)/Fe II(Optical) ratios as a function of microturbulence. For small values of  $v_{turb}$  and with solar abundance, the Fe II(UV)/Mg II ratio is smaller than that of Fe II(UV)/Fe II(Optical). The ratios are the same at  $v_{turb} = 5 \text{ km s}^{-1}$ . However, the Fe II(UV)/Mg II ratio grows faster than that of Fe II(UV)/Fe II(Optical) as a function of microturbulence. The UV Fe II transitions often arise from levels at high excitation energies, and the density of levels increases substantially above 10 eV. Thus, the UV transitions are closer in energy than those in the optical range, and their strengths are more affected by microturbulence than those of optical lines. Although both the Fe II(UV)/Mg II and Fe II(UV)/Fe II(Optical) ratios increase with microturbulence, dependencies are not identical. Our calculations demonstrate that the most reasonable values for Fe II(UV)/Mg II

ratios correspond to  $v_{turb} = 5 - 10 \text{ km s}^{-1}$ .

Is there any specific Fe II feature, line or spectral index in AGN spectra that can be used to derive the iron abundance accurately? To probe the effect of varying abundance, we repeated the calculation with one and five times solar iron abundance, keeping the microturbulence constant at  $v_{turb} = 1 \text{ km s}^{-1}$ . We define the iron abundance sensitivity ratio as  $(I(\text{Fe II})_5 - I(\text{Fe II})_1)/I(\text{Fe II})_1$  and signify integrated fluxes  $I(\text{Fe II})_1$  and  $I(\text{Fe II})_5$  for abundances of solar and five times solar. Calculations with  $v_{turb} = 10 \text{ km s}^{-1}$  (Figure 4) show that this sensitivity ratio has the same slope as it has with  $v_{turb} = 1 \text{ km s}^{-1}$ .

We find that the UV Fe II lines are generally less sensitive to abundance than those in the optical range. Energy levels responsible for UV and optical lines are not populated proportionally with increasing abundance. The structure of the  $\text{Fe}^+$  ion favors the production of more optical emission through cascades from upper levels.

Figure 5 shows how Fe II(UV)/Mg II and Fe II(UV)/Fe II(Optical) emission ratios change with iron abundance (1, 5, and 10 solar). The increase in Fe II (Optical) emission with the Fe abundance is stronger than that in Fe II (UV) emission. Comparisons of radiation and/or turbulence effects confirm that the abundance is not the only factor that affects the Fe II (UV)/Mg II ratio. A factor of 5 in abundance increases the Fe II (UV)/Mg II ratio by factor less than 2. By using Fe II (UV)/Mg II in combination with the Fe II(UV)/Fe II(Optical) emission ratio, we can deduce abundances while accounting for microturbulence and radiation field effects. Table 2 shows predictions for models with different microturbulence ( $v_{turb} = 1 - 100 \text{ km s}^{-1}$ ) and iron abundance (1 – 10 of solar). The columns are the following: microturbulence, abundance, and calculated Fe II(UV)/Mg II and Fe II(UV)/ Fe II(Optical) ratios.

### 3. SUMMARY

By applying the new 830-level model ion for  $\text{Fe}^+$ , which is incorporated into detailed photoionization calculations, we have probed the feasibility of using the strong Fe II emission seen in quasar spectra to derive accurate Fe/Mg abundance enrichments. This Fe II emission would be especially important in determining the enrichment as a function of redshift and the nature of star formation in the Early Universe. We conclude that abundance is not the only factor that makes Fe II emission strong over a wide range of wavelengths and is not even the strongest factor. Our modeling indicates that microturbulence also leads to preferential strengthening of the Fe II emission in UV.

On the basis of the calculations presented here, we make five basic conclusions:

1. In contrast to recent observational Fe II/Mg II measurements, we emphasize the need for low- $z$  quasar observations to calibrate detailed modeling as used here. Our model clearly demonstrates that a simple Fe II template cannot be applied for all quasars, because the Fe II sensitivity to radiation and turbulence is much stronger than that of the Mg II doublet. Only detailed modeling that includes all these effects can provide more accurate Fe II templates.

2. Due to strong Fe II line overlap, we must adopt a wavelength band approach to get constraints on density, radiation field, and turbulence in BLRs. This approach is more complex, but the computational tools are readily available.

3. Further modeling, beyond that presented here, is necessary. Model comparisons with high S/N observations of quasars, and of even higher resolution observations of objects like  $\eta$  Car, will produce better atomic parameters, and more detailed understanding of the effects of the radiation field in astronomical objects. Future work using improved atomic data to fully explore effects of the radiation field is in progress.

4. These results clearly illustrate that the continuum of AGNs is greatly affected by Fe II. The spectrum of Fe II simply cannot be ignored. Understanding Fe II is crucial for obtaining realistic modeling of restframe AGN spectra from the UV through the IR. Studies in the expanded spectral range, much wider than used in any previous efforts, are required.

5. We suggest that our model is to be applied to low-redshift quasars spanning both a wide luminosity range, and the 1,000 – 10,000 Å restframe wavelength range. As the first step in this direction, the STIS and NICMOS capabilities can be used immediately to study low-redshift quasars. The Near Infrared Spectrograph (NIRSpec) on board the James Webb Space Telescope (JWST) would make it possible to measure spectra from 0.6 to 5 micron with resolving power in the range needed to obtain Fe II(UV) and Fe II(Optical) bands from low-redshift to high-redshift quasars.

This research of EV has been supported, in part, through NSF grant (NSF - 0206150) to CUA, and HST GO-08098. EV acknowledge useful discussion with G. Ferland, K. Kawara, and Y. Yoshii. SJ is supported by a grant from the Swedish National Space Board. We wish to acknowledge the use of the computational facilities of the Laboratory for Astronomy and Solar Physics (LASP) at NASA/Goddard Space Center. We give special thanks to Keith Feggs, Don Lindler, and Terry Beck for their computer services support. We thank unknown referee for suggestions that improved the paper.

## REFERENCES

- Dietrich, M., Appenzeller, I., Vestergaard, M., & Wagner, S. J. 2002, ApJ, 564, 581
- Freudling, W., Corbin, M., & Korista, K. 2003, ApJ, 587, L67
- Hamann, F., & Ferland, G. 1993, ApJ, 418, 11
- Hartman, H., & Johansson, S. 2000, A&A, 359, 627
- Heger, A., & Woosley, S. E. 2002, ApJ, 567, 532
- Iwamuro, F., Motohara, K., Maihara, T., Kimura, M., Yoshiii, Y., & Doi, M. 2002, ApJ, 565, 63
- Korista, K., Baldwin, J., Ferland, G., & Verner, D. 1997, ApJS, 108, 401
- Netzer, H., & Wills, B. 1983, ApJ, 275, 445
- Raassen, A. J. J., & Uylings, P. H. M. 1998, A&A, 340, 300
- Verner E. M., Verner, D. A., Korista, K.T., Ferguson, J. W., Hamann, F., & Ferland, G. J. 1999, ApJS, 120, 101
- Verner, E., 2000, Ph.D. thesis, Univ. of Toronto
- Verner, E., Verner, D., Baldwin, J., Ferland, G., & Martin P. 2000, ApJ, 543, 831
- Verner, E. M., Gull, T. R., Bruhweiler, F., Johansson, S., Ishibashi, K., & Davidson, K. 2002, ApJ, 581, 1
- Wheeler, J. C., Sneden, C., & Truran, J. W. 1989, ARA&A, 27, 279
- Wills, B. J., Netzer, H., & Wills, D. 1985, ApJ, 288, 94
- Yoshii, Y., Tsujimoto, T., & Nomoto, K., 1996, ApJ, 462, 266

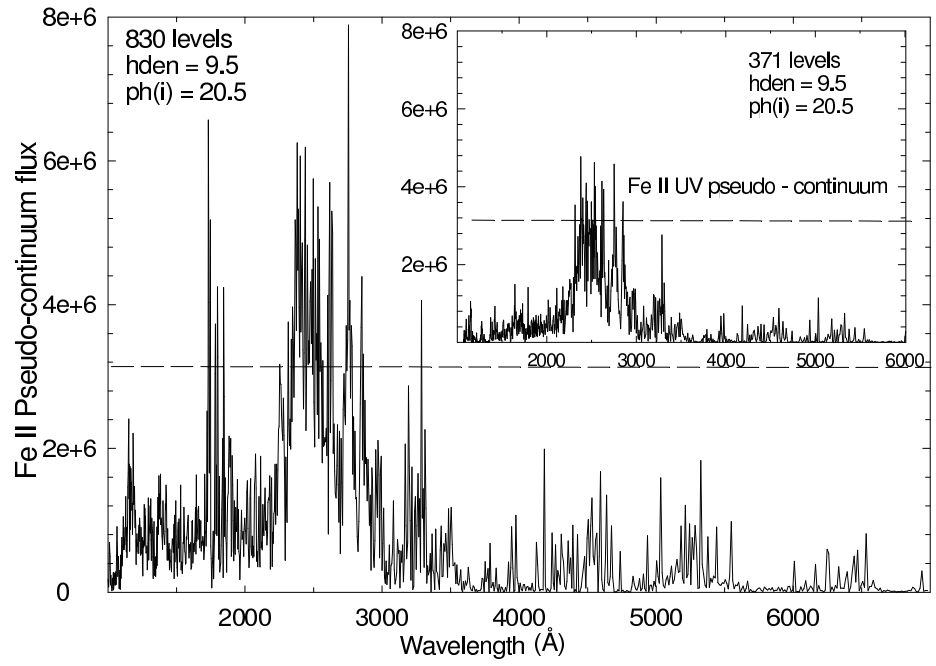
Fig. 1.— Fe II pseudo-continuum predicted by 371 (inset) and 830 level models for Fe<sup>+</sup> in QSOs’ BLR conditions (section 3.1). The 1000–7000 Å wavelength range divided into small bins of 6 Å (consistent with a 500 km s<sup>-1</sup> FWHM at 3600 Å) and Fe II flux calculated in each bin. The total Fe II flux in range 2000–3000 Å increased by factor 1.4 (Table 1) compared to the older model (Verner et al. 1999). The dashed line separates the Fe II pseudo-continuum from strong lines in the 371-level model. The 830-level model predicts many strong Fe II features in the 1600–3500 Å range.

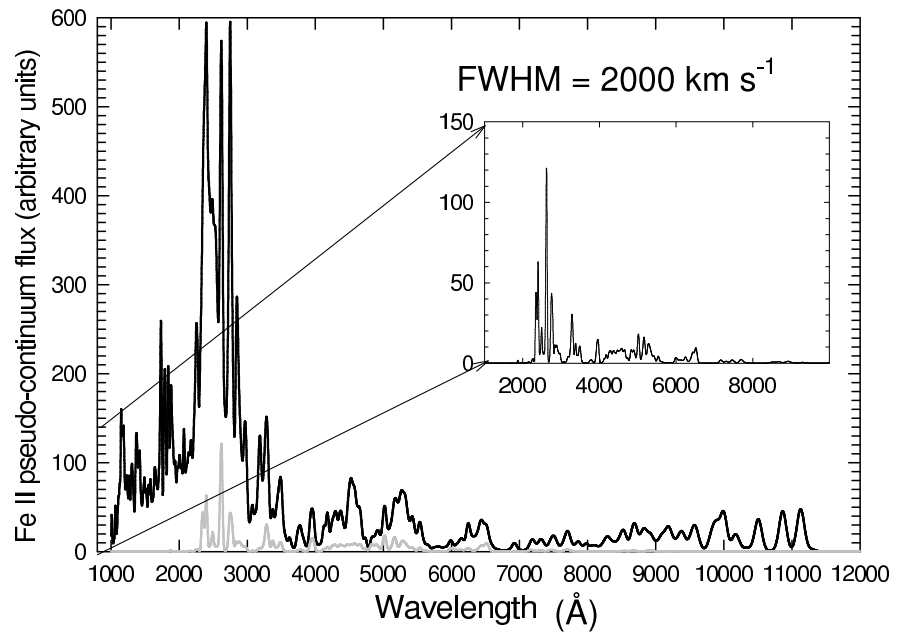
Fig. 2.— Fe II spectrum calculated in a radiative continuum pumping model (solid line) and a pure collisional model (dotted line and inset). Broadening by a non-turbulent FWHM of 2,000 km s<sup>-1</sup> (as observed for broad lines in the quasar 3C 273) has been used to enable comparison with observations.

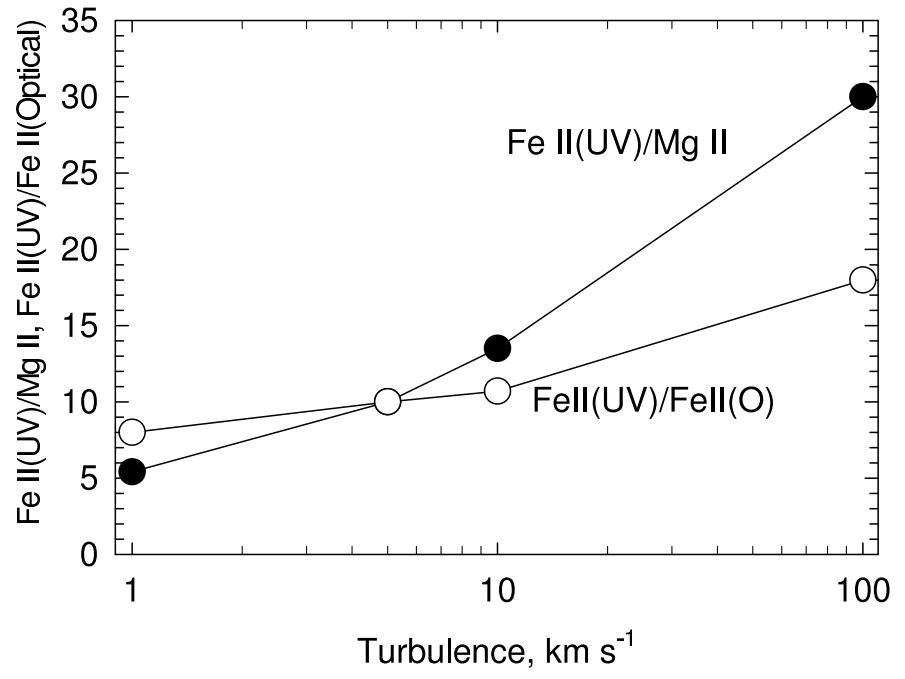
Fig. 3.— Fe II(UV)/Mg II and Fe II(UV)/Fe II(Optical) ratios as a function of microturbulence. See text for further discussion.

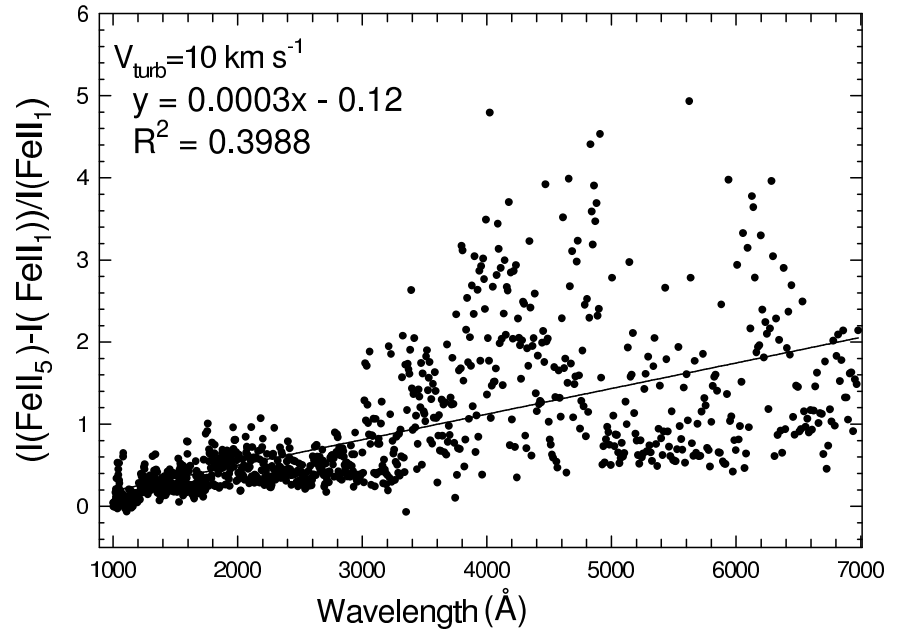
Fig. 4.— The general sensitivity of the Fe II continuum to changes in abundance (for constant  $v_{turb} = 10 \text{ km s}^{-1}$ ). The Fe II(UV) emission is less sensitive to abundance than Fe II(Optical).

Fig. 5.— Fe II(UV)/Mg II and Fe II(UV)/Fe II(Optical) ratios as a function of abundance.









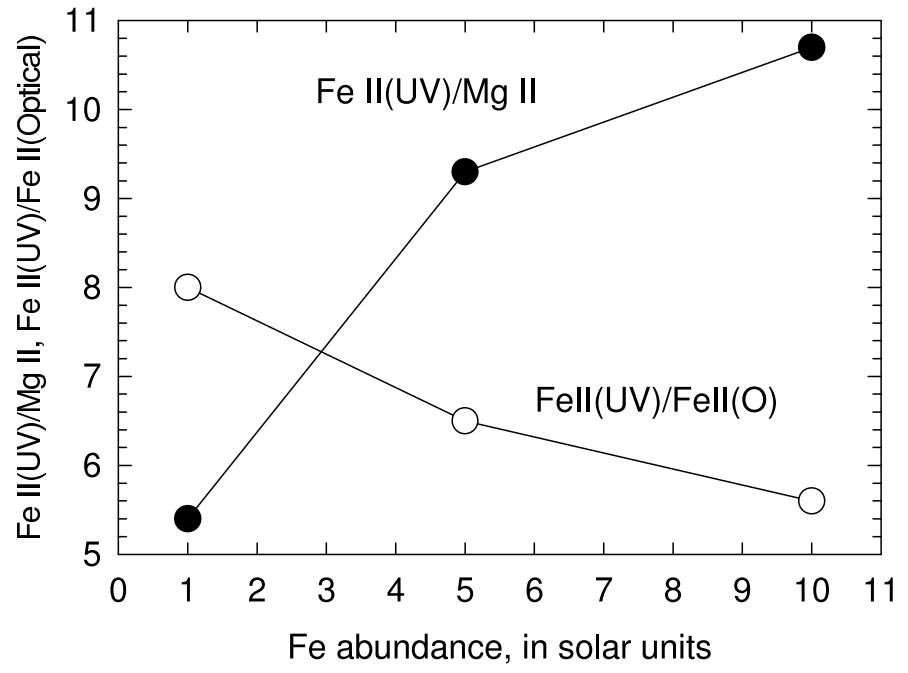


Table 1. Predicted Fe II(UV)/Mg II & Fe II(UV)/Fe II (Optical) Emission Ratios versus Excitation for Solar Abundance and Turbulence of  $1 \text{ km s}^{-1}$ .

Number of levels	Excitation	Fe II(UV)/Mg II	Fe II(UV)/Fe II(Optical)
371	collisional	0.5	2.8
	radiative	4	11.4
830	collisional	0.3	2.8
	radiative	5.4	8

Table 2. Predicted Fe II(UV)/Mg II & Fe II(UV)/Fe II (Optical) Emission Ratios versus Abundance and Turbulence.

Turbulence (km s <sup>-1</sup> )	Abundance	Fe II(UV)/Mg II	Fe II(UV)/Fe II(Optical)
1	1	5.4	8
1	5	9.3	6.5
1	10	10.7	5.6
5	1	10	10
10	1	13.5	10.7
100	1	30	18
5	5	14	6.8
10	5	20	7.3
10	10	27.5	6.4
100	10	77	9.2